Journal of
Nanoscience and Nanotechnology
Vol. 12, 3547–3551, 2012

Fullerene C_{60} Coated Silicon Nanowires as Anode Materials for Lithium Secondary Batteries

Arenst Andreas Arie[2] and Joong Kee Lee[1,*]

[1]*Advanced Energy Materials Processing Laboratory, Energy Storage Center, Korea Institute of Science and Technology, Hwarangno 14-Gil 5, Seongbuk Gu, Seoul 136-791, Republic of Korea*
[2]*Department of Chemical Engineering, Parahyangan Catholic University, Bandung 40141, Indonesia*

A Fullerene C_{60} film was introduced as a coating layer for silicon nanowires (Si NWs) by a plasma assisted thermal evaporation technique. The morphology and structural characteristics of the materials were studied by scanning electron microscopy (SEM) and X-ray photoelectron spectroscopy (XPS). SEM observations showed that the shape of the nanowire structure was maintained after the C_{60} coating and the XPS analysis confirmed the presence of the carbon coating layer. The electrochemical characteristics of C_{60} coated Si NWs as anode materials were examined by charge–discharge tests and electrochemical impedance measurements. With the C_{60} film coating, Si NW electrodes exhibited a higher initial coulombic efficiency of 77% and a higher specific capacity of 2020 mA h g^{-1} after the 30th cycle at a current density of 100 μA cm^{-2} with cut-off voltage between 0–1.5 V. These improved electrochemical characteristics are attributed to the presence of the C_{60} coating layer which suppresses side reaction with the electrolyte and maintains the structural integrity of the Si NW electrodes during cycle tests.

Keywords: Si NWs, C_{60} Coated, Lithium Secondary Batteries, Anode.

RESEARCH ARTICLE

1. INTRODUCTION

Among several alloying materials proposed to replace graphite anodes of lithium secondary batteries, silicon is very promising since it has a theoretical capacity of 4200 mA h g^{-1}.[1] However, silicon materials present two serious problems: huge volume change during alloying/de-alloying processes and low electrical conductivity.[2] This result in the rapid capacity fading during cycle tests which has been the main constraint preventing the commercial application of silicon anodes.[3]

Numerous approaches have been proposed to improve the cycle properties of silicon based anodes, including coating the silicon material with a carbon film, which would maintain the structural integrity of the electrodes as well as increase the electrical conductivity.[4,5] Recently, silicon nanowires (Si NWs), synthesized by metal catalytic etching or chemical vapor deposition (CVD) methods, were proposed as anode materials for lithium ion batteries.[6,7] It is believed that the small diameter (~89 nm) and large number of pores between the wires can compensate the volume expansion that takes place during cycling.[8] However, the large irreversible capacity at the first cycle and the breaking of Si particles into smaller and aggregated forms were still observed for Si NW electrodes after cycling tests.[9,10] These two issues are associated with large internal stress due to the volume expansion and large exposed surface area of Si NWs with the electrolyte, which lead to the formation of an unstable SEI layer on the surface of the Si NW film electrodes.[11]

In this work, fullerene C_{60} films were coated on Si NW films by plasma assisted thermal evaporation techniques and then utilized as anode materials for lithium secondary batteries. To the best of our knowledge, there have been no studies on C_{60} coating on Si NW film electrodes. Our previous works were related to the C_{60} coating of silicon thin films and lithium metal anodes.[12,13] The effects of the C_{60} coating layer on the electrochemical performance of Si NW film electrodes were then investigated.

2. EXPERIMENTAL DETAILS

2.1. Preparation of Si NW Films and C_{60} Film Coating

Si NWs were first grown inside a plasma enhanced chemical vapor deposition (PE-CVD) reactor chamber. Stainless

*Author to whom correspondence should be addressed.

1533-4880/2012/12/3547/005 doi:10.1166/jnn.2012.5557

steel (SS) 316 foil was used as a substrate to grow the Si NWs. Pretreatment of the substrates prior to the deposition included polishing, cleaning and etching using 2% HF solution. After the pretreatment, gold catalyst films were coated onto the SS substrate. Surface treatment of the Au coated SS substrate using hydrogen plasma was also conducted for 20 minutes under the following conditions: working pressure of 75 mTorr, substrate temperature of 580 °C, hydrogen flow rate of 30 sccm and plasma power of 200 W. After the surface treatment, silane (SiH_4) gas was fed into the reactor for the synthesis of Si NWs. Typical operating conditions for the growth of Si NWs were as follows: working pressure of 65 mTorr, substrate temperature of 580 °C, plasma power of 10 W, SiH_4 flow rate of 30 sccm and hydrogen flow rate of 30 sccm. The gas rates were controlled accurately by a mass flow controller (MFC). The growth times were maintained at 1 hour.

The C_{60} coating layer on the surface of the Si NW film was prepared by a plasma assisted thermal evaporation technique using C_{60} powder as a carbon source. C_{60} powder was placed in a tungsten boat set in the center of the evaporation chamber. The chamber was operated at a base pressure of 1.0×10^{-5} Torr by a rotary pump. After heating the C_{60} powder inside the boat, the argon gas was flowed into the evaporation chamber and formed a mixture gas with the evaporated C_{60}. During deposition of the C_{60} thin film on the surface of Si NWs, the working pressure was 2.5×10^{-5} Torr and the plasma powers was 150 W. The substrate temperature was adjusted to a constant value of 150 °C and the films were deposited for 10 minutes.

2.2. Characterizations and Electrochemical Tests

The surface morphology of the films was observed by scanning electron microscopy (SEM-HITACHI) while a compositional analysis was performed by X-ray photoelectron spectroscopy (XPS-VG Scientific).

The electrochemical tests of the film samples were conducted using half cells, which were fabricated by placing a polyethylene separator between the C_{60} coated Si NWs used as a working electrode and lithium metal used as a counter and a reference electrode. The liquid electrolyte was 1 M $LiPF_6$ in ethylene carbonate, ethyl methyl carbonate and dimethyl carbonate (1:1:1 volume ratio). The half cells (2 cm × 2 cm) were then sealed in a polyethylene bag. All the cells were fabricated in a dry room with maximum moisture content of less than 5%. The charge/discharge tests were conducted at current densities of 100 μA cm^{-2}, with a cut off voltage of 0–1.5 V versus Li/Li^+ using a MACCOR battery tester series 4000 at room temperature. The half cells were also studied by electrochemical impedance spectroscopy (EIS-Zahner IM 6) with an amplitude ratio of 5 mV and a frequency range between 0.01 Hz and 10^6 Hz. The surface morphologies of the sample after cycle tests were also observed by SEM. Before the SEM observations, each cell was firstly opened carefully in a dry chamber, washed several times with dimethyl carbonate (DMC) and finally dried in the vacuum oven to remove the volatile components.

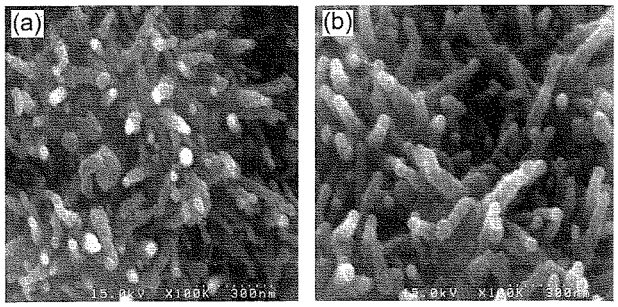

Fig. 1. SEM images of as-deposited (a) bare Si NWs and (b) C_{60} coated Si NW films synthesized on the SS substrate.

3. RESULTS AND DISCUSSION

Figures 1(a and b) show SEM images of the as-deposited bare Si NWs and C_{60} coated Si NW films prepared on the SS substrate, respectively. For both samples, it can be seen that the Si NW films were successfully grown on the substrate. No differences were observed between these two samples, indicating that the shape of the Si NW films was not changed after the C_{60} coating.

Figure 2 shows the XPS spectrum of the as-deposited C_{60} coated Si NWs films. As seen here, the surface of the film sample consists of Si, C and O. The presence of O element might stem from surface contamination due to contact with the air during XPS observations. From the XPS analysis, the atomic concentration on the film surface was also estimated. The sample contained 78% Si, 15% C, and 7% O.

Figure 3 shows the 1st, 5th, 10th, 20th and 30th voltage profiles of bare Si NWs and C_{60} coated Si NW film electrodes at a current density of 100 μA cm^{-2}

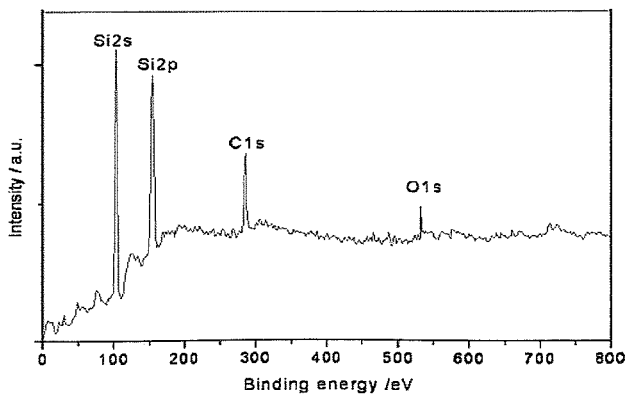

Fig. 2. XPS spectrum of C_{60} coated Si NW films.

RESEARCH ARTICLE

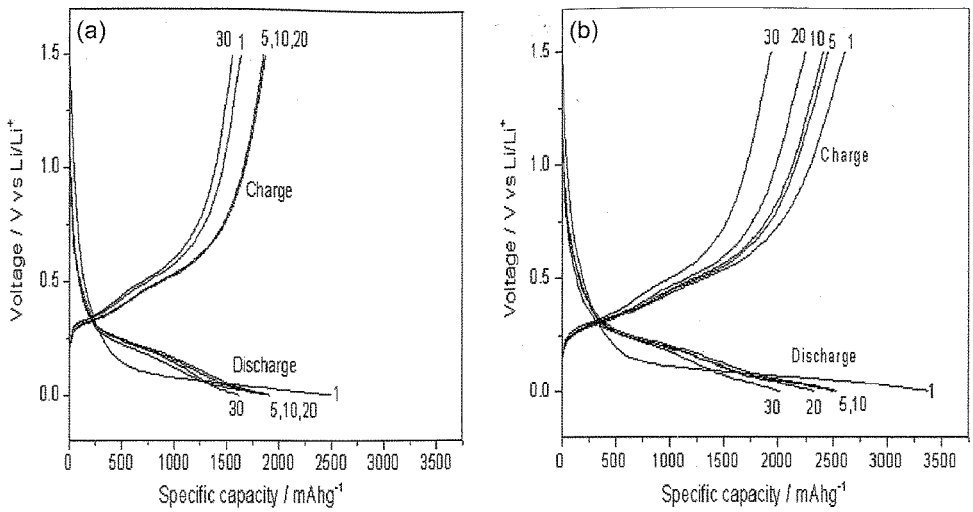

Fig. 3. Voltage profiles of the (a) bare Si NWs and (b) C_{60} coated Si NWs film electrodes at a current density of 100 μA cm^{-2} between 0 and 1.5 V versus Li/Li$^+$.

with a cut off voltage of 0–1.5 V versus Li/Li$^+$. It can be seen that the discharge and charge capacity of the bare Si NW electrodes at the first cycle are 2496.9 and 1632.6 mA h g^{-1}, indicating a large initial irreversible capacity of 864.3 mA h g^{-1}. On the other hand, the C_{60} coated Si NWs electrodes exhibit a discharge capacity of 3377.1 mA h g^{-1} and a charge capacity of 2605.1 mA h g^{-1}, giving an initial irreversible capacity of 772 mA h g^{-1}.

It appears that the C_{60} coating layer on the surface of the Si NWs can slightly reduce the initial irreversible capacity. This improvement is attributed to the suppression of side reactions with the electrolyte and the increased conductivity on the surface of the Si NWs. In general, the voltage profiles for both samples at the first cycle are quite different from those achieved in the following cycles. It may be related to the initial formation of SEI layer on the surface of the electrodes. Additionally, the charge capacity of the bare Si NW electrodes increases with cycling in the initial cycles, indicating that the silicon is not completely active at the beginning of cycling tests. In contrast, the charge capacity of coated sample decreases with cycling, revealing that the presence of the carbon layer could activate the silicon anodes from the beginning.

Figure 4 shows the profiles of the capacity and coulombic efficiency as functions of the cycle number for bare Si NWs and C_{60} coated Si NW film electrodes at a current density of 100 μA cm^{-2}. In general, the bare samples exhibit a lower specific capacity over 30 cycles. At the first cycle, the bare Si NW electrodes show a coulombic efficiency of 65% and discharge capacity of 2496.9 mA h g^{-1}. Finally, the discharge capacity of the bare samples decreases to 1622.8 mA h g^{-1} after the 30th cycle. Meanwhile, the coated samples have a higher discharge capacity of 3377.1 mA h g^{-1} and remain at 2020.2 mA h g^{-1} after the 30th cycle. The coulombic

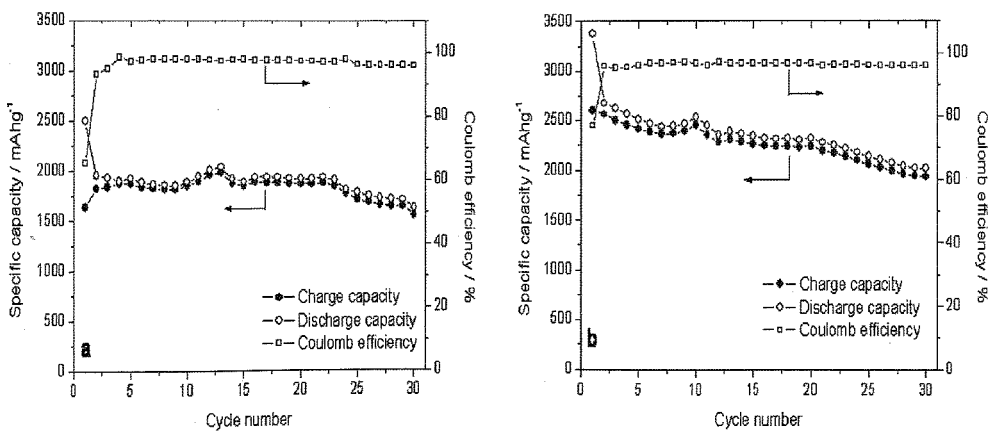

Fig. 4. Profiles of charge–discharge and colulombic efficiency versus cycle number for the (a) bare Si NWs and (b) C_{60} coated Si NW film electrodes at a current density of 100 μA cm^{-2} between 0 and 1.5 V versus Li/Li$^+$.

efficiency of the C_{60} coated Si NWs is about 77% at the first cycle and is maintained above 95% after the first cycle. Clearly, the presence of the C_{60} coating layer elevates the specific capacity and improves the charge–discharge efficiency during the cycle tests. These enhanced electrochemical characteristics may be attributed to the role of the C_{60} film, which allows a formation of more stable solid electrolyte interface (SEI) layer on the surface of the Si NWs electrodes. It appears that the C_{60} film acts both as a good electronic conductor to suppress the side reactions with the liquid electrolyte and as a buffer layer to compensate the effects of volume expansion.

Figure 5 shows the Nyquist impedance spectra of bare Si NWs and C_{60} coated Si NW film electrodes after the 30th cycle, measured in a frequency range between 0.01 and 10^6 Hz. Both of the plots are composed of two overlapped semicircles in the high and middle frequency regions and a straight line in the low frequency region which is related to the Warburg diffusion of lithium ions in the Si NWs.[14] This observation is similar with a previously reported impedance plot for Si NWs.[15] As seen in the figure, the middle frequency semicircle representing the charge transfer process is the dominant part of the spectra. After the 30th cycle, the diameter of this semicircle is much smaller than that of the bare electrode in the case of the electrode coated with C_{60} film. This indicates that the charge transfer resistance is significantly reduced by the presence of the C_{60} coating layer on the surface of the Si NW electrodes. The smaller charge transfer resistance of the coated sample might derive from more stable formation of a SEI layer on its surface due to the suppression of side reactions with the electrolyte.

Figure 6 shows surface SEM images of bare Si NWs and C_{60} coated Si NW electrodes after the 30th cycle. As seen here, the bare Si NWs have aggregated and broken into smaller nano Si particles due to the non-uniform stress generated during the cycling tests.[10] However, the coated Si NWs show a better surface morphology wherein the

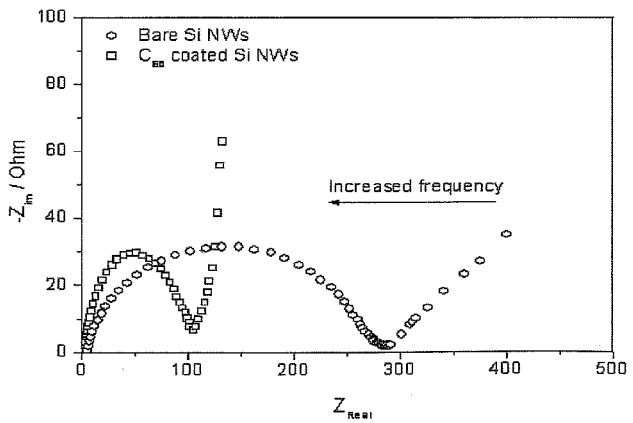

Fig. 5. The Nyquist impedance plots the (a) bare Si NWs and (b) C_{60} coated Si NWs film electrodes after the 30th cycles, measured at the frequency range between 0.01 and 10^6 Hz and amplitude ratio of 5 mV.

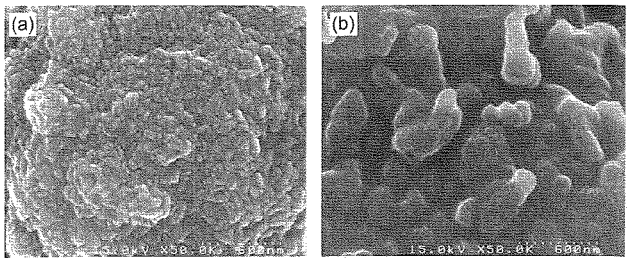

Fig. 6. Surface SEM images of (a) bare Si NWs and (b) C_{60} coated Si NWs electrodes after 30 cycles.

structure of Si NWs can be maintained beyond 30 cycles, indicating that the C_{60} coating layer successfully retains the structural integrity of the Si NW electrodes.

4. CONCLUSIONS

In summary, the Si NW film anodes, coated by a C_{60} coating layer using a plasma assisted thermal evaporation technique, displayed improved electrochemical characteristics in terms of higher initial coulombic efficiency and higher specific capacity over cycling tests. These improved performances are attributed to the presence of the C_{60} coating layer, which enhances conductivity, protects against electrolyte decomposition, and maintains the structural integrity of the electrodes during the insertion and extraction of lithium ions during repeated cycling tests. Future studies will focus on optimization of the C_{60} coating process to achieve further enhanced electrochemical performance including more stable cycle profiles and higher initial coulombic efficiency.

Acknowledgment: This work was supported by the National Research Foundation of Korea Grant funded by the Korean Government (MEST) (NRF-2010-C1AAA001-2010-0028958).

References and Notes

1. U. Kasavajjula, C. S. Wang, and A. J. Appleby, *J. Power Sources* 163, 1003 (**2007**).
2. L. Y. Beaulieu, K. W. Eberman, R. L. Turner, L. J. Krause, and J. R. Dahn, *Electrochem. Solid-State Lett.* 4, A137 (**2001**).
3. M. Yoshio, H. Wang, K. Fukuda, T. Umeno, N. Dimov, and Z. Ogumi, *J. Electrochem. Soc.* 149, A158 (**2002**).
4. J. Xiao, W. Xu, D. Wang, D. Choi, W. Wang, X. Li, G. L. Graff, and J. G. Zhang, *J. Electrochem. Soc.* 157, A1047 (**2010**).
5. L. Su, Z. Zhou, and M. Ren, *Chem. Comm.* 46, 2590 (**2010**).
6. C. K. Chan, R. Ruffo, S. S. Hong, R. A. Huggins, and Y. Cui, *J. Power Sources* 189, 34 (**2009**).
7. B. Laik, L. Eude, J. P. Pereira-Ramos, C. S. Cojocaru, D. Pribat, and E. Rouviere, *Elect. Acta* 53, 5528 (**2008**).
8. C. K. Chan, H. L. Peng, G. Liu, K. Mcllwrath, X. F. Zhang, R. A. Huggins, and Y. Cui, *Nat. Nanotechnol.* 3, 31 (**2008**).
9. R. Huang and J. Xu, *Mat. Chem. Phys.* 121, 519 (**2010**).
10. R. Huang, X. Fan, W. Shen, and J. Xu, *Appl. Phys. Lett.* 95, 133119 (**2009**).

RESEARCH ARTICLE

11. T. Song, J. Xia, J. H. Lee, D. H. Lee, M. S. Kwon, J. M. Choi, J. Wu, S. K. Doo, H. Chang, W. I. Park, D. S. Zang, H. Kim, Y. Huang, K. C. Hwang, J. A. Rogers, and U. Paik, *Nano Lett.* 10, 1710 (**2010**).
12. A. A. Arie, W. Y. Chang, and J. K. Lee, *J. Solid State Electrochem.* 14, 51 (**2010**).
13. A. A. Arie, O. M. Vovk, J. O. Song, B. W. Co, and J. K. Lee, *J. Electroceram.* 23, 248 (**2009**).
14. R. Ruffo, S. S. Hong, C. K. Chan, R. A. Huggins, and Y. Cui, *J. Phys. Chem. C* 113, 11390 (**2009**).
15. X. Chen, K. Gerasopoulos, J. Guo, A. Brown, C. Wang, R. Ghodssi, and J. M. Culver, *ACS Nano* 4, 5366 (**2010**).

Received: 28 October 2010. Accepted: 1 December 2010.